ELSEVIER

Nuclear Physics A616 (1997) 329c–340c

NUCLEAR PHYSICS A

Mass Measurements near N=Z

W. Mittig[1], M. Chartier[1], J. C. Angélique[2], G. Audi[3], J. M. Casandjian[1], A. Cunsolo[4], C. Donzaud[5], M. Chabert[1], J. Fermé[1], L.K. Fifield[10], A. Foti[4], A. Gillibert[11], A. Lépine-Szily[1,6], M. Lewitowicz[1], S. Lukyanov[7], M. Mac Cormick[1], D. J. Morrissey[8], M.H. Moscatello[1], O.H. Odland[13], N. A. Orr[2], A. Ostrowski[1], G. Politi[12], C. Spitaels[1], B. M. Sherrill[8], C. Stephan[5], T. Suomijärvi[5,8], L. Tassan-Got[5], D. J. Vieira[9], A. C. C. Villari[1], J. M. Wouters[9]

1. GANIL, Bld Henri Becquerel, BP 5027, 14021 Caen Cedex, France
2. LPC-ISMRA, Bld du Maréchal Juin, 14050 Caen, Cedex, France
3. CSNSM, Bâtiment 108, 91406 Orsay Cedex, France
4. INFN, Corso Italia 57, 95129 Catania, Italy
5. IPN Orsay, BP 1, 91406 Orsay Cedex, France
6. IFUSP-Universidade de São Paulo, C.P.20516, 14098 São Paulo, Brasil
7. LNR, JINR, Dubna, P.O. Box 79, 101 000 Moscow, Russia
8. NSCL, MSU, East Lansing MI,48824-1321, USA
9. LANL, Los Alamos NM, 87545, USA
10. Dep. of Nucl. Phys., RSPhySE, Austr. Nat. Univ., ACT 0200, Australia
11. CEA/DSM/DAPNIA/SPhN, CEN Saclay, 91191 Gif-sur-Yvette, France
12. Universitá di Catania, Dip. di Fisica, Corso Italia 57, 95125 Catania, Italy
13. Universitetet i Bergen, Fysisk Institutt, Allégaten 55, 5007 Bergen, Norway

Abstract

After an outline of the physics motivations, that illustrate why we think it is important to measure masses in the region N≈Z, we report on on experiments performed at Ganil. An experiment aimed at measuring the masses of proton-rich nuclei in the mass region A ≈ 60-80 has been performed, using a direct time-of-flight technique in conjunction with SISSI and the SPEG spectrometer at GANIL. The nuclei were produced via the fragmentation of a ^{78}Kr beam (73 MeV/nucleon). A novel technique for the purification of the secondary beams, based on the stripping of the ions and using the α and the SPEG spectrometers, was succesfully checked. It allows for good selectivity without altering the beam quality. Secondary ions of ^{100}Ag, ^{100}Cd, ^{100}In and ^{100}Sn were produced via the fusion-evaporation reaction ^{50}Cr + ^{58}Ni at an energy of 5.1 MeV/nucleon, and were accelerated simultaneously in the second cyclotron of GANIL (CSS2). About 10 counts were observed from the production and acceleration of ^{100}Sn^{22+}. The masses of ^{100}Cd, ^{100}In and ^{100}Sn were measured with respect to ^{100}Ag using the CSS2 cyclotron, with precisions of 2×10^{-6}, 3×10^{-6} and 10^{-5} respectively.

PII: S0375-9474(97)00104-8

1 Symmetries near N=Z

Different motivations may be relevant for the study of nuclei near N=Z. Amoungst them we may cite the following:

- Shell-closures
  If shell closures occur in N=Z nuclei, this means automatically that we have a doubly magic nucleus. Study of double magic nuclei and the nearby nuclei has always been one of the the testbench for nuclear models. On the N=Z line the last relatively well studied nucleus is ^{56}Ni. Since one year ^{100} Sn was reached and is now available for experimental studies. The mass-measurement of this nucleus will be discussed below. This will be the last doubly magic nucleus that may be studied, the heavier ones being predicted to be unstable with respect to particle emission by all models.

- Deformations
  The fact that N=Z assures that proton and neutron deformations will be equal and they will enhance each other. This is why the strongest deformations of the nuclear chart are expected around the N=Z line. This can be seen for example in the overview of deformations calculated in the relativistic mean field approach by [1], where very strong deformations are predicted around N≈Z≈40, with fast transitions between oblate and prolate deformations [2]. This was one of the mativations for γ spectroscopy in this region, as is described in [3].

- Symmetries
  Isospin being a good quantum number, nuclei around N=Z should be related by simple symmetries. A particularly simple example are mirror nuclei, this is nuclei having N+x,Z and N,Z+x neutrons and protons respectively, with N=Z. Very precise tests were possible in these cases: as an example we may cite Coulomb displacement energies. For x=1 the binding energy of the neutron and proton is different by, to first order, the Coulomb energy of the extra-nucleon in the field of the core. Knowing the charge distribution of the core and the wave function of the extra-nucleon, this can be calculated precisely. The result is the so called Nolen-Schiffer anomaly, this is the calculations do not agree with experiment. Most recent calculations[4, 5] including charge symmetry breaking interactions,mainly due to mixing of ω and ρ mesons were able to reduce the difference, but in the mirror nuclei ^{17}F-^{17}O and ^{41}Ca-^{41}Sc a significant difference remains that seems to increase with mass. Extension of measurements to much heavier nuclei is therefore desirable.

- Wigner term
  For nuclei around N=Z a supplementary binding energy arises from the neutron-proton pairing, giving a much stronger contribution in this case than elsewhere. This is often called the Wigner term. This term can be associated to a SU(4) symmetry, as was recently shown by [7]. It depends on the existence of spin-isospin independant forces. It can be extracted from double binding energy differences[8]. On figures 1 these pairing energies are shown for odd-odd nuclei, using experimental masses from the Audi-Wapstra[33, 6] tables. As can be seen, there is a much stronger pairing energy for N=Z; the difference between the pairing energy for N=Z as compared to N≠Z is about 3MeV for light nuclei,

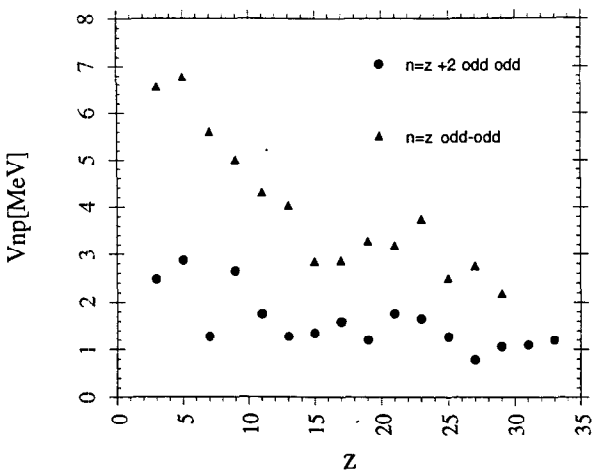

Figure 1: *Neutron-proton pairing energy for odd-odd nuclei for N=Z and N=Z+2.*

and goes down to about 1.5MeV for the heaviest nuclei where this information is available, A≈60. Angular momentum and Coulomb interaction will destroy this SU(4) symmetry, however it is not clear at the moment how fast this term will disappear with increasing mass. It was suggested [7] that there may exist pseudo-SU(4) symmetries, that might result in a strong Wigner term for heavier nuclei. Experimental and theoretical investigations are therefore necessary to clarify this question. This is a longstanding problematic (see for exemple[20]). Improofed experimental conditions should allow us to progress in this domain.

2 Measurements for A≈60-80

Interest in this region has also stemmed from the role played by these nuclei in astrophysical events such as x- and γ-ray flashes [9]. In particular, the drip-line (and near drip-line) nuclei in this region are believed to provide the pathway at high mass for the so-called rapid proton (rp-) capture process [10] (at lower mass, A $< \sim$ 40, the pathway is adjacent to the line of stability). This process is believed to take place in environments, such as the accretion of material onto a neutron star from a companion in a binary system, during explosive hydrogen burning [11]. Recent studies [12, 13, 14] have begun to map the drip-line in this mass region and thus provided constraints on the possible pathways and termination point of the rp-process. Scant experimental information is available on the masses of the nuclei in this region [6], particularly at the drip-line itself. This is due for the most part to the difficulty in producing the nuclei - for nuclei below A $\approx$ 60 the masses are better known due to their proximity to the line of stability. Presently the results of global calculations and systematics of the nuclear mass surface are used to estimate the various reaction rates involved in modelling the rp-process (proton capture, photodisintegration and β-decay). Measuring the masses of key-nuclei at the drip-line or close

to it is thus vital for accurate modelling of the rp-process [11], as relevant Q-values can be determined.

2.1 Experimental procedure

It has been demonstrated by earlier experiments [12, 16] that a relatively high energy, high intensity ^{78}Kr beam and a mass separator can be used to reach these nuclei. In the present experiment a ^{78}Kr beam at 73 MeV/nucleon was hitting a 90 mg/cm^2 thick ^{nat}Ni target located between the two solenoids of SISSI (Source d'Ions Secondaires à Solénoides Supraconducteurs Intenses). The choice of a Ni target was based on earlier results which demonstrated that nucleon transfer is still important at these energies (note, for example, that isotopes of both Rb and Sr were produced from a ^{78}Kr beam [12]). The reaction products were subsequently selected (see below) using the alpha-shaped beam analysis device (α-spectrometer) near the cyclotron CSS2 and transported to the focal plane of the SPEG spectrometer.

The mass measurement technique has been used in a series of previous experiments by our group [17, 18, 26] which to date have concentrated on lighter neutron-rich nuclei. The method exploits the long flight-path (~100 m) available between the α-spectrometer and the SPEG spectrograph. A measure of the magnetic rigidity ($B\rho$), the time-of-flight (TOF), and the atomic number and the charge state (q) of the ions in a flight path of length (L) of an achromatic system. The mass (m) of the ions can thus be deduced from the expression :

$$B\rho = \frac{m}{q} \cdot \frac{L}{TOF} \tag{1}$$

The achromatic system comprises the beam line after the production target up to the focal plane of SPEG [17, 18, 26] .

Given the resolution of the method (of the order of 2×10^{-4} in order to reach a final uncertainty of ~ 250 keV or better, a total yield of $\sim$ 1000 events or more counts will be necessary for a given nucleus.

2.2 Secondary Beam Purification by Strippping

We used a high energy, high intensity ^{78}Kr beam and a Ni target to produce secondary beams that were then guided through to SPEG. More than 200 different nuclei are produced in this reaction. This corresponds to a production rate of $5 - 7 \times 10^5$ pps according to estimations given by the codes INTENSITY and LISE. On the one hand our detectors could not bear such high counting rates, and on the other hand the maximum beam intensity was required to produce the more exotic nuclei.Thus it was absolutely necessary to purify the secondary beams.

A thin layer ($\sim$ 1 mg/cm^2) of Ta was evaporated on the downstream face of the target in order to increase the yield of ions produced in the $q = Z - 1$ charge state. Additionally a thin mylar stripping foil ($\sim$ 1 mg/cm^2) was mounted between the two dipole stages of the α-spectrometer

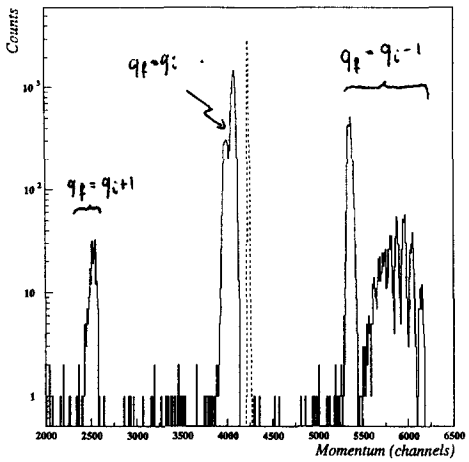

Figure 2: *A secondary beam containing different charge states, as observed on the dispersive focal plane of SPEG. The broken line shows the momentum distribution of the beam without any foil, the full line shows the same beam when a thin foil($\approx 1mg/cm^2$) is put in the beam line before the spectrometer. The different changes of charge states are now separated specially,and can be selected by a slit. Note that in this example the most important process is the pick up of one electron.*

in order to strip the last electron. Using asymmetric settings of the two sections of the α-spectrometer this provided not only for the elimination of the more prolific lighter nuclei, but also a strong selectivity based on the atomic number of the ions.
Consider :

$$B\rho_1 = \frac{mv}{q_1} \tag{2}$$

and

$$B\rho_2 = \frac{mv}{q_2} \tag{3}$$

for the setting of the first and second parts of the α-spectrometer, with, in this case,$q_1 = Z - 1$ and $q_2 = q_1 + 1 = Z$. This change in $B\rho$ allows for the selection of one charge state, which is equivalent to the selection of *one* Z, since the nuclei are fully stripped after the foil.This method is illustrated on figure 2 , where the momemtum spectrum with and without a thin charge changing foil is illustrated.

Importantly the present method provides a very good selectivity without altering the beam quality. Data analysis is in progress, and it is envisaged that the masses of ^{71}Br and $^{68,70}Se$ may be determined with a good precision, while those of ^{70}Br, ^{67}Se, ^{65}As and ^{63}Ge will have

a somewhat lower precision due to lower statistics. Improvements are also expected in existing mass determinations in this region.

3 Mass measurements in the region of ^{100}Sn

The doubly-magic nucleus ^{100}Sn was recently produced and identified in two independent experiments using the projectile fragmentation technique : at GSI with a 1.1 GeV/nucleon ^{124}Xe beam [21] and at GANIL using a 63 MeV/nucleon ^{112}Sn beam [22]. Due to its N = Z character at the double shell closure, there was much effort to reach this nucleus, and its observation represents the culmination of many years of effort. However, its observation demonstrates only that it is bound against proton decay whereas a measurement of its mass provides more detailed information. Our final aim is the determation of the eventual existence of a a Wigner term in this region.
The method available for measuring masses of nuclei produced in fragmentation reactions employs time-of-flight over a linear flight path of $\sim 50 - 100$ m [17, 23, 18, 24, 25, 26] , using high precision magnetic spectrometers (SPEG [27] at GANIL and TOFI [28] at Los Alamos). With currently available count rates, the resolution of these devices is not good enough to perform precise mass measurement of ^{100}Sn. Given the much increased path length when the ions follow a spiral trajectory, we have developed a method using the second cyclotron of GANIL (CSS2) as a high precision spectrometer. The mass resolution obtained with the simultaneous acceleration of A/q = 3 light ions (^{6}He, ^{9}Li) was shown to be 10^{-6} [29, 30].

In the present work, ^{100}Sn nuclei, together with nuclei of ^{100}Ag, ^{100}Cd and ^{100}In were produced by a fusion-evaporation reaction and accelerated simultaneously. The mass resolution achieved with these heavy ions was of the order of 3×10^{-5}. Using the mass of ^{100}Ag as a reference, the masses of ^{100}Cd, ^{100}In and ^{100}Sn could be determined with precisions (depending on the statistics) of 2×10^{-6}, 3×10^{-6} and 10^{-5} respectively.

Details of the method used with light ions have already been published [30], so here we will concentrate on features specific to the present work. The method consists in substituting the existing stripper located between the two cyclotrons by a production target, in which the secondary nuclei are produced and are subsequently injected into and accelerated by CSS2.

Neutron-deficient A = 100 nuclei were produced by fusion-evaporation reactions between a ^{50}Cr^{9+} beam accelerated by the CSS1 cyclotron and a ^{58}Ni target. This reaction is known to be very favourable for the production of nuclei around ^{100}Sn [31]. The highest cross-section is for the production of ^{100}Ag, followed by ^{100}Cd and ^{100}In. Using the Monte-Carlo codes PACE and HIVAP, the optimal energy for the production of ^{100}Sn was estimated to be 255 MeV.

Accelerated ions were detected inside the cyclotron using a silicon detector telescope (ΔE 35, E 300μm) mounted on a radial probe which can be moved from the injection radius (1250 mm) up to the extraction radius (3000 mm). The time-of-flight, or phase (one RF period being equal to 360°), of the detected ions was measured relative to the RF signal of the CSS2 cyclotron.

For two nuclei, masses m and $m + \delta m$, accelerated simultaneously in CSS2, the separation in time, δt, after N_T turns is given to first order by :

$$\frac{\delta t}{t} = \frac{\delta m}{m} \tag{4}$$

where t is the total transit time, $t = N_T.h_2/f$, and f is the frequency of the accelerating voltage.This relation is the basis of the calibration procedure : the unknown mass $m + \delta m$ can be determined from the well known reference mass m if the number of turns N_T or the total time-of-flight t are known.

In order to separate genuine ^{100}Sn events from background, a particle identification parameter $f(Z)$, proportional to the atomic number Z, was derived from a linear combination of the signals from the two detectors of the silicon detector telescope. The coefficients were determined empirically from the data by varying the total energy of the products detected in the silicon detector telescope (related to the radial position of the probe). Figure 3 shows a plot of this identification parameter versus phase. The horizontal lines mark off the regions where the bulk of each ion species is to be found. Note that, in the region of phase around -10° where the ^{100}Sn events are expected, there is a scattered background of events in the Ag and Cd windows, very few in the In window, and several events in the Sn window. There is an excess of 10-12 events in the Sn spectra of Figure 3 around -10° which have correct phase, total energy and $f(Z)$ value simultaneously, and these are attributed to $^{100}Sn^{22+}$ ions. The relative intensities of these Ag and Cd events in the In and Sn spectra respectively differ by a factor of ten. If it is assumed that the background near -10° is due to Ag and Cd ions, then this background would be expected to scale accordingly. Since there are only 4 background counts in the In spectrum, the expected background in the Sn spectrum is therefore no more than 1 count. For a more detailed discussion see [37].

In order to determine the masses of the various isobars it is necessary to determine their centroids in phase. This was accomplished using an iterative procedure to subtract the Ag contribution from the Cd spectrum, the Ag and Cd contributions from the In spectrum, and the Ag, Cd and In contributions from the Sn spectrum to arrive at fairly pure spectra (in the anticipated region of phase) for each of the four isobars, from which the centroids could be determined. The number of turns before detection, N_T, which was required to turn the time differences between the various isobars and ^{100}Ag into mass differences, according to equation 4, was determined in a separate measurement at the conclusion of the experiment. Finally, we arrive at the following mass excesses :

$$M.E.(^{100}Cd) = -74.180 \pm 0.200(syst.)MeV$$

$$M.E.(^{100}In) = -64.650 \pm 0.300(syst.) \pm 0.100(stat.)MeV$$

$$M.E.(^{100}Sn) = -57.770 \pm 0.300(syst.) \pm 0.900(stat.)MeV$$

The systematic uncertainties take account of the uncertainties in the subtraction procedure described above. We supposed that there were no long-lived isomeric states. These masses are to be compared with the experimental values presented in the Audi-Wapstra mass table [6] for

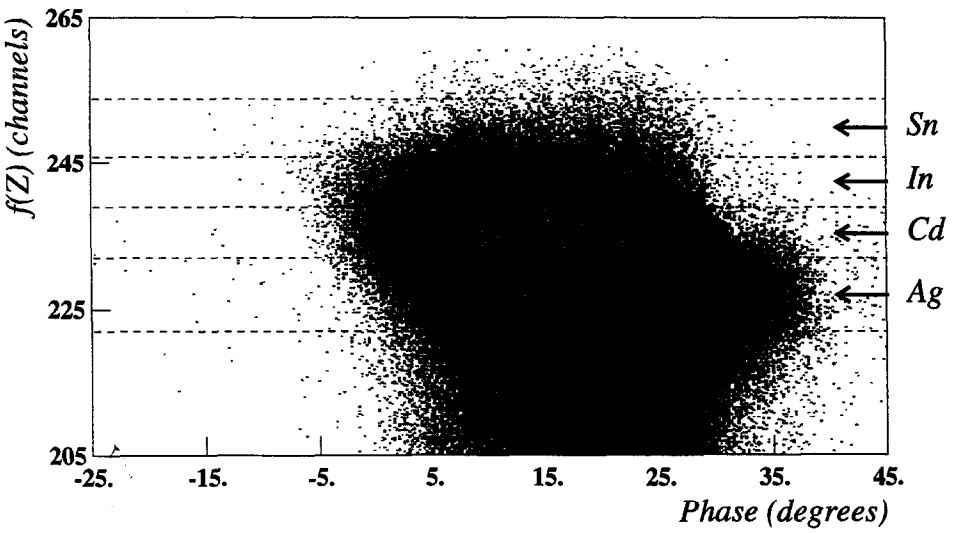

Figure 3: *Identification parameter f(Z) versus phase spectrum (see text). In this spectrum, we can set different gates corresponding to four f(Z) regions attributed to Ag, Cd, In and Sn. The big vertical tail, coming from channeling effect in the ΔE detector, has no influence on the good events.*

^{100}Cd (-74.310 ± 0.100 MeV) [34] and also for ^{100}In (-64.130 ± 0.380 MeV) which was obtained from the combination of an indirect measurement [35] and our previous direct measurement using the CSS2 cyclotron technique [36]. The mass of ^{100}Sn (-56.860 ± 0.430 MeV) given in the Audi-Wapstra mass table [6] is an estimate based on extrapolating systematic trends. Our mass of ^{100}Cd is in good agreement with the existing measurement, which gives good confidence in the new results for ^{100}In and ^{100}Sn.

We compared the shell model calculations of Johnstone and Skouras [39] to the Audi-Wapstra mass table [6] for the binding energies of isotones N = 50, 51 and 52 (see Figure 4). We can see that the calculations and the values of the table are in good agreement as far as experimental data are available (up to ^{98}Ag and ^{100}Cd). But there is a clear disagreement when the mass table values are derived by extrapolating systematic trends. On Figure 4 are represented 33 nuclei from ^{90}Zr to ^{102}Sn. We added on the same graph our experimental results for ^{100}Cd, ^{100}In and ^{100}Sn (represented by black stars). As is visible, the shell model calculations agree well with our results, predicting a stronger binding energy than the extrapolations from systematics. An overbinding could be due to a Wigner term. Of course, the present result is not sufficiant to give a final answer on this question: it is not clear what is really contained in the extrapolation by systematics. It is clear that it does not contain a Wigner term, but it may have other deficiencies. We hope,too, that the present data and other data on mid-shell nuclei presently being analysed will contribute to answer this question. Further progress can be expected by both experimental and theoretical work. As stated in the introduction, the Wigner

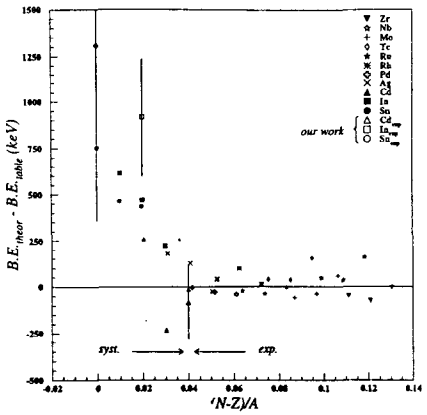

Figure 4: *Comparison between the shell model calculations of Johnstone and Skouras [39] ($B.E._{theor}$) and the mass table of Audi and Wapstra [15] ($B.E._{table}$) for the binding energies of isotones $N \pm 50$, 51 and 52 from ^{90}Zr to ^{102}Sn. The binding energies of the mass table come either from experimental values (right side of the dashed vertical line) or from systematic trends extrapolations (left side of the line). Our experimental results are represented by black stars.*

term can be determined by double binding energy differences[8], thus involving quadruplets of nucei. In the case of ^{100}Sn, this involves ^{96}Cd and ^{98}Cd, the mass of ^{98}Sn could be deduced from the mirror nucleus ^{98}Cd. Calculations over a larger domain around N = Z = 50 would be desirable, too, in order to disentangle different effects. For exemple the shell model calculations of ref.[39] do not contain enough nuclei in order to extract the theoretical double binding energy differences related to the Wigner term.

3.1 Comparison of Fragmentation and Fusion Evaporation Reactions.

We may compare our experimental count rates to statistical model calculations. As noted above, the absolute transmission of the CSS2 is difficult to determine. However, if we suppose that the mean charge distribution for the different isobars is centered approximately at the same value (which could be wrong, e.g. if delayed Auger electron emission changed strongly the charge state after the target), we can obtain relative cross-sections. To our knowledge, only one value has been measured [38] for ^{100}Ag, which is 3.9 mb. This value is one order of magnitude lower than estimations from statistical model calculations that we used previously to estimate the absolute cross-section. If we normalize our count rates to this experimental value [38] for ^{100}Ag, we obtain the cross-sections of Table 1, all of which are an order of magnitude lower than the statistical model predictions.

Note that the small 40 nb cross-section for ^{100}Sn is nonetheless three orders of magnitude larger than the ones in fragmentation reactions [21, 22]. We used our result, and the compilation of [3], in order to compare the cross-sections of these two reaction cross sections, see figure 5. We converted yields of N=Z nuclei by fragmentation reactions of [12, 13, 14] to cross sections in order to establish a general trend. Note that this conversion is not very precise, implying transmission rates of spectrometers. None the less the general tendancy is clear: cross sections of fusion evaporation reactions are about 3 orders of magnitude higher than the ones

	Present Work		Stat. Model	Stat. Model	Stat. Model
	(c/h/nAe)	(mb)	PACE (mb)	HIVAP (mb) [31, 40]	CASCADE (mb)
^{100}Ag	~ 40	3.9 [38]	30	38	38
^{100}Cd	~ 10	~ 1	16	7	3.2
^{100}In	~ 0.01	~ 0.001	0.02	0.014	0.027
^{100}Sn	$\sim 4 \times 10^{-4}$	$\sim 4 \times 10^{-5}$	-	0.0003	-

Table 1: *Experimental cross-sections of the present work normalized to the value of Schubart et al [38] for ^{100}Ag, and compared to statistical model calculations.*

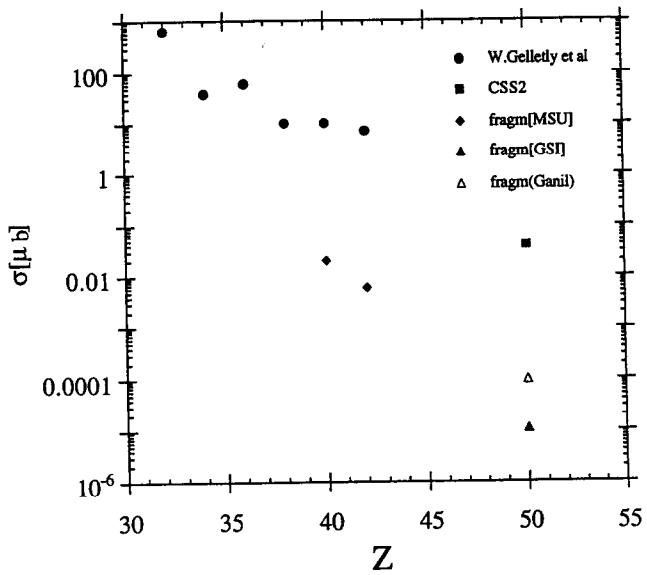

Figure 5: *Production cross section of N=Z nuclei.*

of fragmentation, thus compensating the much thinner useful target thickness possible.

4 Conclusion

We have performed two experiments for the mass measurement of nuclei with N≈Z. The purification by charge state change in thin foils was succesfully tested. In this region of the nuclear chart, fusion evaporation reactions are very competitive with respect to fragmentation reactions. They should be considered, too, for the preparation of Isol beams. ^{100}Sn has been observed as the product of a fusion-evaporation reaction for the first time using the CSS2 cyclotron of GANIL as an efficient high precision mass spectrometer. The masses of not only ^{100}Sn, but also ^{100}In and ^{100}Cd were determined using ^{100}Ag as a reference. The known mass excess of ^{100}Cd has been confirmed within 2×10^{-6} and we measured for the first time the masses of ^{100}In and ^{100}Sn with a precision of 3×10^{-6} and 10^{-5} respectivly. A preliminary production cross-section of 40 nb has been determined for the fusion-evaporation reaction ^{50}Cr + ^{58}Ni $\longrightarrow$ ^{100}Sn at 255 MeV.

References

[1] D.Hirata et al, RNB4, Omaya 1996, present proceedings

[2] C.J. Lister et al , Phys.Rev. **C42**, 1191 (1990).

[3] W. Gelletly, Acta Physica Pol. **B26**, 323 (1995).

[4] T.Suzuki,H.Sagawa and A.Arima, Nucl.Phys. **A536**, 142 (1992).

[5] L.N.Epele et al., Phys.Lett. **B277**, 33 (1992).

[6] G. Audi and A.H. Wapstra , Nucl.Phys. **A595**, 409 (1995).

[7] P.Van Isacker, D.D.Warner, and D.S.Brenner, Phys.Rev.Lett. **74**, 4607 (1995)

[8] D.S.Brenner, C.Wesselborg, R.F.Casten,D.D.Warner and J.-Y.Zhang, Phys.Lett. **B243** 1 (1994).

[9] R.E. Tamm , Ann. Rev. Nucl. Part. Sci. **35**, 1 (1985).

[10] R.K. Wallace and S.E. Woosley , Ap. J. Suppl. **45**, 389 (1981).

[11] A.E. Champagne and M. Wiesher , Ann. Rev. Nucl. Part. Sci. **42**, 39 (1992).

[12] M.F. Mohar et al , Phys. Rev. Lett. **66**, 1571 (1991).

[13] S.J. Yennello et al , Phys. Rev. **C46**, 2620 (1992).

[14] B. Blank et al , Phys. Rev. Lett. **74**, 4611 (1995).

[15] G. Audi and A.H. Wapstra , Nucl.Phys. **A565**, 1 (1993).

[16] J.A. Winger et al , Phys. Lett. **B299**, 214 (1993).

[17] A. Gillibert et al , Phys.Lett. **B176**, 317 (1986).

[18] A. Gillibert et al , Phys.Lett. **B192**, 39 (1987).

[19] N.A. Orr et al , Phys.Lett. **B258**, 29 (1991).

[20] J.M.D'Auria, J.W.Gruter, L.Westergaard, G.Nyman, P.Peuser, E.Roeckl, H.Otto, Proc. 3rd Int. Conf. on Nuclei far from Stability, Cargese, CERN **76-13** (1976).

[21] R. Schneider, J. Friese, J. Reinhold, K. Zeitelhack, T. Faestermann et al, Z.Phys. **A348**, 241 (1994).

[22] M. Lewitowicz, R. Anne, G. Auger, D. Bazin, C. Borcea et al, Phys.Lett. **B332**, 20 (1994).

[23] D.J. Vieira, J.M. Wouters, K. Vaziri, R.H. Kraus Jr., H. Wollnik et al, Phys.Rev.Lett. **57**, 3253 (1986).

[24] J.M. Wouters, R.H. Kraus Jr., D.J. Vieira, G.W. Butler and K.E.G. Löbner, Z.Phys. **A331**, 229 (1988).

[25] X.L. Tu, X.G. Zhou, D.J. Vieira, J.M. Wouters, Z.Y. Zhou et al, Z.Phys. **A337**, 361 (1990).

[26] N.A. Orr, W. Mittig, L.K. Fifield, M. Lewitowicz, E. Plagnol et al, Phys.Lett. **B258**, 29 (1991).

[27] L. Bianchi, B. Fernandez, J. Gastebois, A. Gillibert, W. Mittig et al, Nucl.Instr.Meth. **A276**, 509 (1989).

[28] J.M. Wouters, D.J. Vieira, H. Wollnik, G.W. Butler, R.H. Kraus Jr. et al, Nucl.Instr.Meth. **B26**, 286 (1987).

[29] G. Auger, W. Mittig, A. Lépine-Szily, L.K. Fifield, M. Bajard et al, Nouvelles du GANIL **50**, 7 (1994).

[30] G. Auger, W. Mittig, A. Lépine-Szily, L.K. Fifield, M. Bajard et al, Nucl.Instr.Meth. **A350**, 235 (1994).

[31] E. Roeckl, private communication (1994).

[32] G. Auger, W. Mittig, A. Lépine-Szily, M. Chartier, D. Bibet et al, Nouvelles du GANIL **54**, 7 (1995).

[33] G. Audi and A.H. Wapstra, Nucl.Phys. **A595**, 409 (1995).

[34] K. Rykaczewski, A. Płochocki, I.S. Grant, H. Gabelmann, R. Barden et al, Z.Phys. **A332**, 275 (1989).

[35] J. Szerypo, M. Huyse, G. Reusen, P. Van Duppen, Z. Janas et al, Nucl.Phys. **A584**, 221 (1995).

[36] A. Lépine-Szily, G. Auger, W. Mittig, M. Chartier, D. Bibet et al, Proceedings of the ENAM 95 Conference on Exotic Nuclei and Atomic Masses, Arles, France, June 19-23 (1995).

[37] M. Chartier, G. Auger, W. Mittig, A. Lépine-Szily, et al, Preprint Ganil P96-16, and to be published

[38] R. Schubart, H. Grawe, J. Heese, H. Kluge, K.H. Maier et al, Z.Phys. **A352**, 373 (1995).

[39] I.P. Johnstone and L.D. Skouras, Phys.Rev. **C51**, 2817 (1995).

[40] K. Rykaczewski, private communication (1995).